

STB-SASB: Combining Synthetic Aperture Sequential Beamforming with Synthetic Transmit Beams for Wireless Ultrasound Probes

Pascal Alexander Hager*, Luca Benini*[†]

*Integrated Systems Laboratory (IIS), ETH Zurich, Switzerland, {hager, benini}@ethz.ch

[†]Electrical, Electronic, and Information Engineering, University of Bologna, Italy

Abstract—Wireless ultrasound probes typically perform beamforming on the probe and communicate B-mode images to meet bandwidth constraints of wireless links. Performing on-probe beamforming is thermally-bound, hence wireless probes typically only provide limited capabilities compared to cart-based systems.

In this work, we apply Synthetic Aperture Sequential Beamforming (SASB) to enable beamforming "after" the wireless link, i.e., on the mobile device connected with the wireless probe. SASB enables wireless transmission of the data by performing only simple operations on the probe. The compute-intensive part of the image formation is performed on the connecting device. However, SASB consumes much energy in the analog front-end compared to other methods such as diverging beams imaging.

In this paper, we present the first (to the best of our knowledge) working prototype of a 64-channel wireless ultrasound probe performing SASB. The prototype allows comparing the energy-consumption and image quality of SASB with other methods. To improve the energy-consumption, we propose STB-SASB, a combination of SASB with synthetic transmit beams (STB). STB-SASB with two synthetic beams reduces the front-end consumption by 50% with ideal power management. On our system, we demonstrate savings of 31% with a minor quality degradation of 6% in resolution (FWHM). More synthetic beams reduce the consumption even further at the cost of quality.

Index Terms—Synthetic Transmit Beams, Synthetic Aperture Sequential Beamforming, Wireless Ultrasound Imaging

I. INTRODUCTION

Digital ultrasound probes embed the entire transmit- and receive front-end within the enclosing of the transducer probe and provide a digital interface to the connecting system. Today, digital probes are widely used in tablet/smartphone-based portable imaging systems, where a digital probe is connected to a smartphone over USB or Wireless LAN (WiFi).

In order to lower cost and increase flexibility, it is desirable to transfer the raw data directly to the tablet/smartphone to perform image formation on its GPU. This allows leveraging the newest mobile processors, which are generally based on the most advanced and energy-efficient CMOS technology (e.g. 7 nm). However, the raw data cannot be easily transferred to the mobile device as WiFi/USB cannot handle the several Gbit/s of data the front-end produces: The raw RF data of five channels (12 b, 20 MS/s) already exceeds 1 Gbit/s. Therefore most digital probes perform all or part of the image formation (beamforming) on the probe and send out B-mode images. Unfortunately, the probe electronics cannot be fabricated in

the most advanced digital CMOS processes, as production volumes would not justify design and production costs.

Moreover, the thermal design budget for the electronics integrated into the probe is limited, as the probe's surface temperature may not exceed 43°C (IEC60601-1). A large share of the available thermal budget has to be invested into the transmit- and receive front-end, which typically consumes 40-100 mW/channel [1]. Current probes thus use low-volume high-unit-cost hardware (ASICs), manufactured in non-leading edge CMOS technology, to compute the image as energy-efficiently as possible to fit into the remaining thermal budget. These thermal constraints on the number of front-end channels and feasible processing complexity limit the capabilities of such portable systems compared to large cart-based systems.

Synthetic Aperture Sequential Beamforming (SASB) [2] addresses some of these issues with a two-stage beamforming scheme to increase the capabilities of portable systems: A low-complexity beamformer in the probe reduces the data before sending it to the smartphone, where a second-stage GPU beamformer computes the image [3]. SASB supports B-mode [4] and vector flow [5]. However, SASB does not address the energy dissipation of the analog front-end itself.

In this work, we present the first (to the best of our knowledge) working prototype of a 64-channel wireless ultrasound probe performing SASB. The first-stage beamformer is implemented on an Artix-7 FPGA in the probe, and the result is sent over WiFi to a PC for second-stage beamforming. We use the prototype to assess the energy-efficiency of SASB and compare it to other methods. To improve the energy-efficiency, we propose a new imaging method (STB-SASB), which combines SASB with synthetic transmit beams (STB) [6]. STB-SASB allows reducing the duty-cycle of the ultrasound front-end by 2× with minimal quality degradation.

II. WIRELESS IMAGING SYSTEM WITH SASB

Fig. 1 shows the system overview of the wireless ultrasound imaging system performing SASB imaging. The system consists of a probe connected wirelessly to a host system.

For the probe hardware, we are using our digital ultrasound probe, LIGHTPROBE [7]. LIGHTPROBE is a 64-channel 4 MHz phased-array probe that embeds the entire transmit-receive front-end in the probe handle. It is powered at 5 V with max. 3 A (compatible with USB powering) and can output the

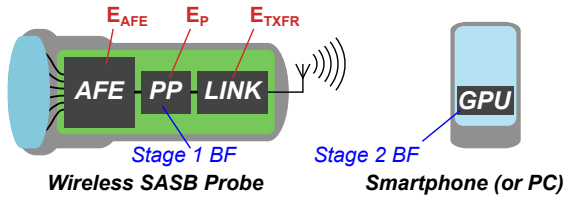


Fig. 1. Overview of a wireless ultrasound imaging system using SASB: The wireless probe captures the raw data using its RX/TX analog front-end (AFE) and pre-processes (PP) the raw data using a low-complexity beamformer (BF) before transmitting (LINK) the data to a connecting device. The connecting device performs a second beamforming step on its GPU.

captured data either over a WiFi-module (IEEE 802.11b/g/n) or a high-speed (up to 26.4 Gb/s) fiber optics link (powered off in the wireless configuration used in this paper). It contains a Xilinx Artix 7 FPGA that allows deploying different processing hardware in the probe. In this work, the low-complexity first-stage SASB beamformer and our STB extension thereof are implemented on the Artix 7 FPGA.

For the host system, we use an off-the-shelf PC to perform the second-stage beamforming and display the image. It has been previously shown in [3] that an HTC Nexus 9 Tablet connected to a research scanner emulating a wireless probe can perform second-stage SASB beamforming for vector flow imaging at up to 26 frames/s. These specifications can be easily exceeded by recent products using more advanced Systems-on-chip: the 2014 Nvidia Tegra K1 SoC used in the Nexus 9 is roughly $10\times$ less powerful than the Tegra Xavier SoC, the latest chip produced in 2019 by Nvidia for the same market.

III. DESIGN CONSIDERATIONS FOR WIRELESS IMAGING

When designing an imaging method for a wireless system, the following considerations should be taken into account:

First, the amount of data per frame D [bit] that needs to be transferred to the host system must be sustainable by the link rate L [bit/s] for the target frame rate f [Hz], i.e., $D \cdot f \leq L$.

Second, the energy dissipated in the probe per frame $E_{\text{Frame}} = E_{\text{AFE}} + E_{\text{P}} + E_{\text{TXFR}}$ must be thermally sustainable. The three contributors are the front-end energy E_{AFE} , required to emit the ultrasound pulse and receive the echos, the processing energy E_{P} , required to reduce the amount of raw data, and the transfer energy E_{TXFR} , required to move the data to the host. Assuming a 30 Hz frame rate and a thermal budget of 5 W, E_{Frame} is upper bounded by 166 mJ/Frame. For a wireless link, we can expect an energy dissipation in the probe of 10 nJ/bit (802.11n/ac) for transmitting data [8]. If we allocate at most 2 W of the thermal budget to the link, the link rate L is upper bounded by 200 Mbps. This implies that D must be less than 0.83 MB for 30 Hz imaging. The energy contribution for processing is usually the least critical, as digital processing can be implemented very energy-efficiently in ASICs [9]. In order to fit into the thermal budget, no more than 1 W should be spent for processing. Thus, at most 3 W (100 mJ/Frame) remain for the front-end. In an ideal system, E_{AFE} is $Q \cdot E_{\text{Shot}}$, where E_{Shot} is the energy spend in the ultrasound front-end (TX-Pulser, ADC, ...) for one ultrasound transmit/receive cycle and Q the number of acquisitions required to compose a frame.

- Thus, an ideal imaging method for a wireless system has:
- 1) low energy dissipation in the front-end, i.e., $Q \cdot E_{\text{Shot}} < 100$ mJ. This is easiest achieved with a small Q .
 - 2) little data (<1 MB) to be transferred per frame.
 - 3) a processing dissipation in the probe of less than 1 W.

IV. STB-SASB

A. Synthetic Aperture Sequential Beamforming (SASB)

SASB [2] imaging works as follows: The transmit sequence is equal to conventional imaging, where each image line (scanline) is acquired by emitting a pulse focused to a point (transmit focal point) on that line. The number of required shots Q is equal to the number of scanlines. SASB applies two beamforming steps to compute the image points: First, a fixed-focus beamformer is applied with a fixed receive focus to the transmit focal point. The output of the first beamformer, called *low-resolution-line (LRL)*, can be considered as the signal response of *virtual transducer element* emitting spherical waves, located at the transmit focal point. With this interpretation, the Q LRLs computed from the Q acquisitions can be viewed as the raw data of a monostatic synthetic aperture acquisition [10] using a *virtual array* with its elements placed at the transmit focal points. Therefore, the LRL data can be fed to a second, synthetic aperture beamformer. Since synthetic aperture beamformers can emulate dynamic *transmit* beamforming, the image quality of SASB is significantly better than conventional methods [4].

SASB allows placing the first low-complexity beamformer in the probe and the second high-complexity beamformer in the connecting device. The first beamformer implicitly compresses the data by a factor equal to the number of channels N . While SASB reduces D , it does not reduce Q .

Since our probe is equipped with a phased array, we use a version of SASB for phased arrays (P-SASB) [11].

B. Synthetic Transmit Beams (STB)

There are several ways to reduce the number of shots Q : One approach is to acquire only every I -th scanline. Assuming the system was initially critically sampled according to the Rayleigh criterion, it will cause image quality degradation due to under-sampling. Another technique is parallel receive beamforming [12], i.e., capture several scanlines with just one emission. This technique is prone to create artifacts in the image [6]. These artifacts are removed with a method called synthetic transmit beams (STB) [6], where synthetic scanlines are interpolated from neighboring scanlines.

As elaborated in [6], in the case of marginal sampling and equal aperture on transmit and receive, two parallel beams ($I = 2$) can be created per emission without causing under-sampling. We will focus on this case in the paper. In the results section, we will briefly elaborate cases for $I > 2$.

C. Combining STB with SASB

To benefit from the low D of SASB and the ability of STB to reduce Q , we propose to combine both techniques to reduce the number of shots for SASB by a factor of I . We will

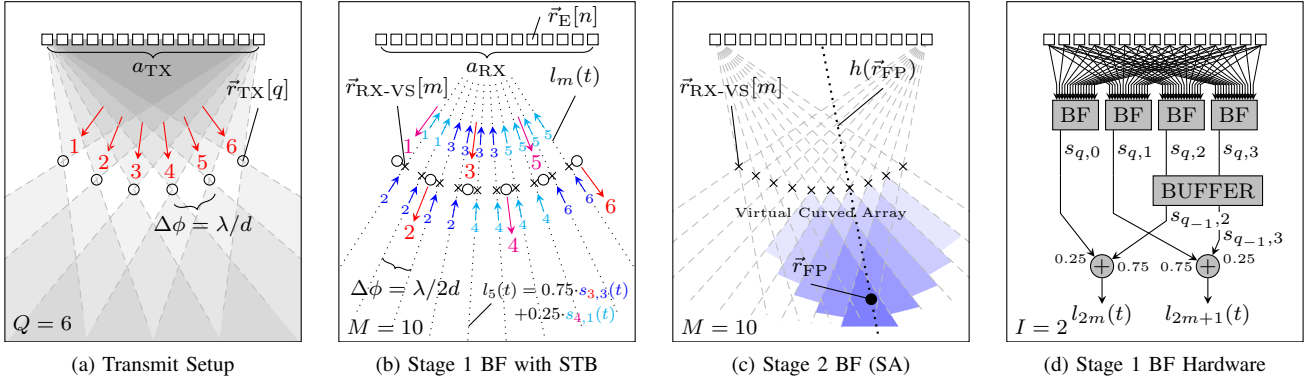


Fig. 2. STB-P-SASB imaging with $I = 2$: (a) Transmit setup: $Q = 6$ acquisitions are sequentially performed with the transmit-focus $\vec{r}_{TX}[q]$ placed on an arc at fixed focal depth from the transducer center point. (b) First stage beamforming (BF) with STB: for each acquisition (red/magenta) $2I = 4$ synthetic scanlines (blue/cyan) are beamformed in parallel. The numbers indicate which lines are beamformed for which transmission. The low-resolution lines $l_m(t)$ are interpolated from two coinciding synthetic lines. (c) Second stage synthetic aperture (SA) beamforming by reinterpreting the $l_m(t)$ as data from a virtual curved array, with its elements at the receive focal points $\vec{r}_{RX-VS}[m]$ of the stage 1 BF. (d) Hardware implementation of the first stage BF with STB: $2I = 4$ fixed focus beamformers operate in parallel. $I = 2$ LRLs are computed per shot to be sent to the connecting system for second stage beamforming.

interpolate $M = (Q - 1) \cdot I$ LRLs out of Q acquisitions. As in [6] we offset the placement grid of the synthesized scanlines such that no interpolated scanline coincides with an actual transmit beam. This results in a more homogeneous interpolation.

In the following, we will explain the transmit setup, the first stage beamforming combined with STB, and the second stage beamforming. For more details on STB and SASB see [2], [6]. Fig. 2 shows the geometrical setup for STB-P-SASB.

1) *Transmit Setup* (Fig. 2a): Q acquisitions are performed sequentially. The transmit focal points $\vec{r}_{TX}[q]$ are placed on an arc in front of the transducer with $\Delta\phi = \lambda/a_{TX}$ spacing to satisfy the *one-way* Rayleigh criterion. The receive signal $r_{n,q}(t)$ of all transducers are captured in every shot q .

2) *First Stage Beamforming with STB*: (Fig. 2b): For each shot q , $2I$ synthetic scanlines (I on each side of the TX-beam)

$$s_{q,j}(t) = \sum_n r_{n,q}(t - d(\vec{r}_E[n], \vec{r}_{RX-VS}[j])) \quad (1)$$

are computed using a fixed-focus receive beamformer, i.e., the delay function d is independent of depth/time. The M receive focal points $\vec{r}_{RX-VS}[m]$ are placed at the same depth as the transmit focus, but with a tighter spacing $\Delta\phi = \lambda/(a_{TX} + a_{RX})$ to satisfy the *two-way* Rayleigh criterion. The low-resolution SASB scanlines $l_m(t)$ are then computed with a linear combination (interpolation) from the two synthetic scanlines (s_{q,j_1}, s_{q+1,j_2}) that geometrically coincide with l_m (see Fig. 2b):

$$l_m(t) = w_1 \cdot s_{q,j_1}(t) + w_2 \cdot s_{q+1,j_2}(t). \quad (2)$$

The weights w are chosen to correspond to the relative distance of $s_{q,j}(t)$ to the transmit beam center of shot q , i.e., $w_j \in \{0.25, 0.75\}$ in the case of $I = 2$. See [6] for details.

3) *Second Stage Beamforming* (Fig. 2c): As previously elaborated, the SASB LRL can be viewed as the raw data of a monostatic synthetic aperture signal acquisition using a *virtual array* with its elements placed at $\vec{r}_{RX-VS}[m]$. The synthetic

aperture high-resolution image $h(\vec{r}_{FP})$ can thus be computed with standard dynamic delay and sum beamforming, i.e.,

$$h(\vec{r}_{FP}) = \sum_m^M g(m, \vec{r}_{FP}) \cdot l_m(d(\vec{r}_{RX-VS}[m], \vec{r}_{FP})). \quad (3)$$

The function $g(m, \vec{r}_{FP})$ selects which virtual elements $\vec{r}_{RX-VS}[m]$ can contribute to \vec{r}_{FP} from the geometrical situation and applies a Hanning apodization over the selected elements. The function returns 0 for elements not contributing. See [11] for details. Fig. 2c shows in blue shades, the area of contribution for the elements contributing to an exemplary focal point. The focal points between the actual array and the virtual array can be computed by backward focusing. This requires the delay function d to compute distances with a negative value when the focal point is behind the virtual array.

D. On-Probe HW Implementation of Stage 1 BF with STB

The STB-SASB first stage beamformer computes I LRL per shot from the raw data of the $N = 64$ receive channels. Fig. 2d shows the hardware implementation placed in the wireless probe. $2I$ parallel fixed-focus beamformers are required. The result (1) of the first I beamformer is combined with the buffered result of the other I beamformer from the previous shot (2). In order to minimize buffer size and data for wireless transmission, the output is compressed with demodulation and decimation [9]. The resulting LRL lines are sent over WiFi to the connecting device for second stage beamforming (3).

V. EXPERIMENTAL SETUP

To compare the front-end energy dissipation E_{AFE} and image quality of SASB and STB-SASB, we operate the LIGHTPROBE in a tethered configuration, where the probe is connected to a PC over the optical link [13]. This allows to capture the entire raw received data from the front-end and process it without implementation loss or slow-down. All measurements are performed for 30 Hz imaging. The front-end is turned off between frames to save energy [7]. The processing

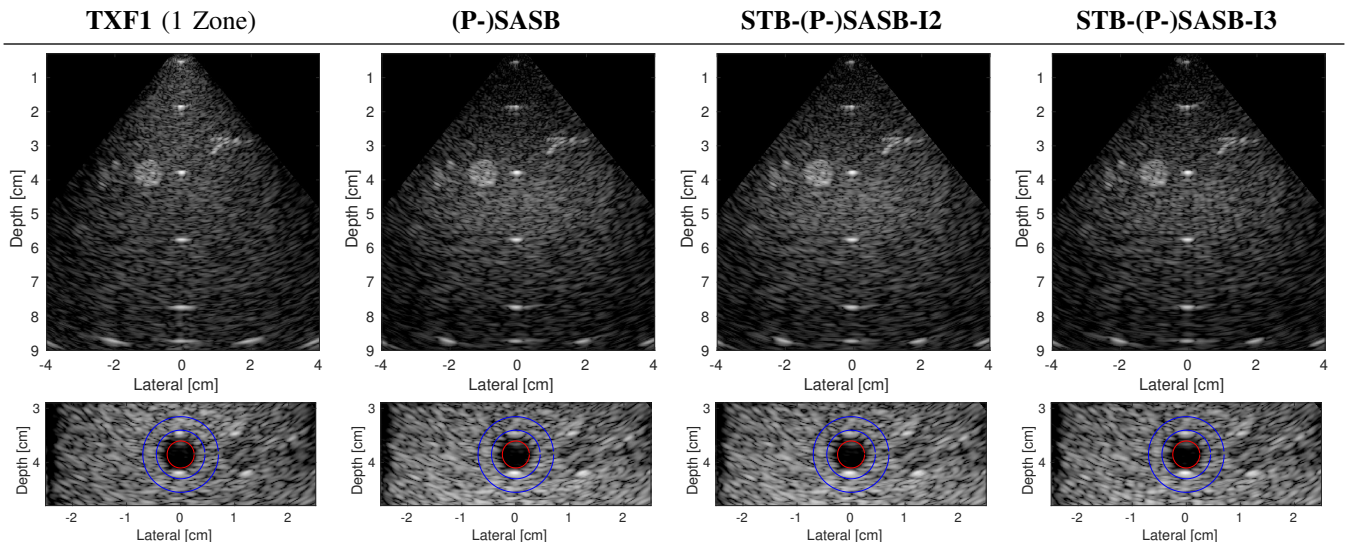


Fig. 3. Image quality comparison of single-zone imaging (TXF1), P-SASB and our STB-P-SASB method. For STB-P-SASB, we show the output image for $I=2$ (-I2) and $I=3$ (-I3). The latter violates the Rayleigh criterion resulting in stripe-artifacts. Images are shown in 50 dB (upper row) and 40 dB (lower row).

power E_P is estimated with a differential measurement with and without deploying the first-state SASB beamformer on the FPGA. For the measurements, a CIRS 054GS phantom is used with a 4 MHz 2-period ± 50 V transmit pulse, and 20 MHz receive sampling. The used setup is exactly the same as in [7] to enable comparison. In this work, we are evaluating the following strategies in detail:

TXF1 Conventional sequential imaging with 91 scanlines and fixed transmit focus at 5 cm (78° field-of-view).

P-SASB Phased array synthetic aperture sequential beamforming with the same scanlines/transmit focus as TXF1.

STB-P-SASB-I2 P-SASB using STB with 2 synthetic beams per transmit. Same TX setup as TXF1 but performing only every second acquisition (46 shots).

STB-P-SASB-I3 P-SASB using STB with 3 synthetic beams per transmit. Same TX setup as TXF1 but performing only every third acquisition (31 shots).

VI. RESULTS

A. Image Quality (Resolution & Contrast)

Fig. 3 shows the scan-converted and log-compressed output images. The numerical results are in Tbl. I. As expected P-SASB improves the average resolution over TXF1: The average full width at half maximum (FWHM) of the point targets on the centerline is improved from 2.61° to 2.18° (16%) at the cost of contrast (-0.96 dB). Our proposed STB-P-SASB-I2 method with 2 beams per transmit shows no visible difference to P-SASB despite using only half the number of acquisitions. There is a tiny difference in resolution (0.13° , 6%) and contrast (+0.24 dB). STB-P-SASB-I3 with a transmit beam spacing of $\Delta\phi = 3/2 \cdot \lambda/a_{TX}$ to reduce the number of shots by $3\times$ compared to a critically sampled TXF1, violates the two-way Rayleigh criterion resulting in stripe-artifacts. Artifacts can be avoided for $I > 2$ at the cost of resolution by reducing the size of the active aperture a_{TX} during transmit. A smaller active aperture would also reduce E_{AFE} .

TABLE I
COMPARISON RESULTS

Method	Q	D [MB]	L [Mbit/s]	E_{AFE} [mJ]	FWHM	CNR
TXF2*	182	35.8	8587.8	205	2.41°	7.58 dB
TXF1	91	17.9	4293.9	128	2.61°	7.60 dB
VS13*	13	2.6	613.4	69	2.69°	7.03 dB
SASB	91	0.28	67.1	131	2.18°	6.64 dB
STB-SASB-I2	46	0.28	67.1	91	2.32°	6.88 dB
STB-SASB-I3	31	0.28	67.1	78	2.24°	7.11 dB

* The results for multi-zone imaging (TXF2) and divergent beams (VS13) are taken from [7].

B. Energy & Link Rate

Tbl. I lists for all methods the data per frame, the link rate, and the front-end energy dissipation for 30 Hz imaging. Fig. 4 plots L vs. E_{AFE} . Only the SASB-based methods have a sufficiently low D (0.28 MB) to support wireless transmission (67.1 Mbit/s @ 30 Hz) within our power budget. The estimated link power is 0.671 mW. On our prototype system, the conventional methods (TXF1, TXF2), as well as standard SASB, consume too much energy per frame in the front-end (>100 mJ) to stay within our 3 W thermal budget. In contrast, divergent beam imaging (VS13, 13 shots per frame) consumes half the energy (69 mJ/Frame) with only minor quality degradation (-22% FWHM, +5% CR) compared to SASB. Divergent beam imaging requires a huge link rate (>1 Gbit/s) and on-probe beamforming is unfeasible as it requires 91x-parallel-beamforming with dynamic delays. Combining SASB with STB reduces the front-end consumption into the thermally feasible region (91 mJ/Frame, <3 W @ 30 Hz).

C. SASB Prototype

Our SASB wireless probe (Fig. 5) is fully operational and currently achieves a frame-rate of 1.5 Hz. The used low-power WiFi module (RAK439) only supports 6 Mbit/s, which limits the framerate to 2.7 Hz. Much faster rates are supported by more recent low-power modules (e.g. Cypress's CYW4343W).

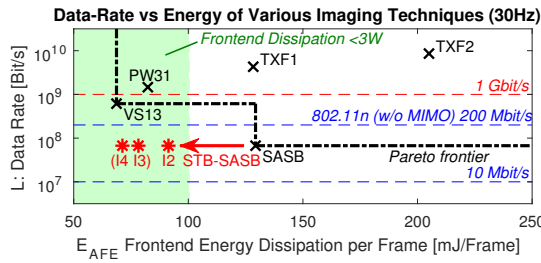


Fig. 4. Comparison of measured off-probe data-rate and front-end energy dissipation between SASB and other imaging techniques put into context with feasible power dissipation (thermal constraints) and link rates (wireless). In red, improvements when combining SASB with STB.

The first-stage beamformer with STB-support for up to $I = 3$ (six fixed-focus beamformers) dissipates 0.85 W on the FPGA, confirming that SASB is a lightweight pre-processing operation. The SASB block utilizes 28 k LUT, 37 k Registers, 466 DSPs and 36 BRAM on the Artix-7 FPGA. The largest share (19.5 k LUT, 27 k REG, 448 DSP) is used for sub-sample interpolation to support fractional delays in (1).

VII. DISCUSSION

While SASB (67.1 Mbit/s) enables wireless transmission, its front-end dissipation (131 mJ/Frame) is too high for thermal constraints. Other methods (VS13) meet thermal constraints but exceed wireless rates. Combining SASB with STB reduces the front-end consumption into the thermally feasible region (91 mJ/Frame, $<3\text{ W}$ @ 30 Hz), with a minor quality degradation of 6% FWHM for two synthetic beams. More beams reduce energy even further at the cost of quality.

Previous work [5], [14], [15] focused on demonstrating that mobile devices provide sufficient compute power for wireless imaging. The required probe was only emulated. In this work, we present a first prototype of the missing probe. Actual measurements provide insight on what energy consumption is to be expected for various imaging methods. With STB-SASB, we present an imaging method especially optimized for wireless imaging.

Our prototype is a truly mobile system as we can forward the image computed on the PC to any mobile device. This enables us to carry around the probe within wireless range freely. In that sense, we demonstrate *cloud*-beamforming. Considering upcoming low-latency mobile network standards (5G), the wireless probe could send the data into the cloud or a server in the building of the healthcare provider, where unconstrained processing power is available to support even the most compute-intensive (CNN-based) algorithms on a wireless system.

VIII. CONCLUSIONS

We have presented a first demonstrator of a wireless probe performing SASB imaging. Our proposed imaging method combining SASB with STB allows reducing the energy consumption in the front-end by up $2\times$ with minor quality impact. In our prototype system, we demonstrated energy-savings by 31%, making STB-SASB feasible on our system.



Fig. 5. Our wireless probe and a smartphone displaying in real-time the forwarded SASB image computed on a PC connected to the same network. The probe is powered over USB with a battery pack visible in the background.

ACKNOWLEDGMENTS

We thank Matthias Bragger for his contributions to the prototype system. The LIGHTPROBE project was funded by Nano-Tera.ch with Swiss Confederation financing.

REFERENCES

- [1] T. Di Ianni *et al.*, "System-level Design of an Integrated Receiver Front-end for a Wireless Ultrasound Probe," *IEEE Trans. Ultrason., Ferroelectr., Freq. Control.*, vol. 63, no. 11, pp. 1935–1946, 2016.
- [2] J. Kortbek *et al.*, "Sequential beamforming for synthetic aperture imaging," *Ultrasonics*, vol. 53, no. 1, pp. 1–16, 2013.
- [3] T. Di Ianni *et al.*, "Real-time implementation of synthetic aperture vector flow imaging on a consumer-level tablet," *IEEE International Ultrasonics Symposium, IUS*, vol. 2, pp. 1–4, 2017.
- [4] M. C. Hemmsen *et al.*, "In vivo evaluation of synthetic aperture sequential beamforming," *Ultrasound in medicine & biology*, vol. 38, no. 4, pp. 708–16, 2012.
- [5] T. D. Ianni *et al.*, "A Vector Flow Imaging Method for Portable Ultrasound Using Synthetic Aperture Sequential Beamforming," *IEEE Trans. Ultrason., Ferroelectr., Freq. Control.*, vol. 64, no. 11, pp. 1655–1665, 2017.
- [6] T. Hergum *et al.*, "Parallel Beamforming Using Synthetic Transmit Beams," *IEEE Transactions on Ultrasonics, Ferroelectrics, and Frequency Control*, vol. 54, no. 2, pp. 271–280, 2007.
- [7] P. A. Hager and L. Benini, "LightProbe: A Digital Ultrasound Probe for Software-Defined Ultrafast Imaging," *IEEE Transactions on Ultrasonics, Ferroelectrics, and Frequency Control*, vol. 66, no. 4, pp. 747–760, 2019.
- [8] D. Halperin *et al.*, "Demystifying 802.11n Power Consumption," *Proceedings of the 2010 Workshop on Power Aware Computing and Systems (HotPower'10)*, pp. 2–6, 2010.
- [9] P. A. Hager *et al.*, "Ekho: A 30.3W, 10k Channels Fully-Digital Integrated 3D Beamformer for Medical Ultrasound Imaging Achieving 298.1M Focal Points per Second," *IEEE Transactions on Very Large Scale Integration (VLSI) Systems*, vol. 24, no. 5, pp. 1936–1949, 2015.
- [10] J. T. Ylitalo and H. Ermert, "Ultrasound Synthetic Aperture Imaging: Monostatic Approach," *IEEE Trans. Ultrason., Ferroelectr., Freq. Control.*, vol. 41, no. 3, pp. 333–339, 1994.
- [11] D. Bera *et al.*, "Synthetic Aperture Sequential Beamforming for Phased Array Imaging," *2015 IEEE International Ultrasonics Symposium, IUS 2015*, no. 1, pp. 1–4, 2015.
- [12] D. Shattuck *et al.*, "Explososcan: A parallel processing technique for high speed ultrasound imaging with linear phased arrays," *Journal of the Acoustical Society of America*, vol. 75, no. 4, pp. 1273–1282, 1984.
- [13] P. A. Hager *et al.*, "UltraLight: An Ultrafast Imaging Platform based on a Digital 64-Channel Ultrasound Probe," in *IEEE Ultrasonics Symposium Proceedings*, 2017.
- [14] M. C. Hemmsen *et al.*, "Implementation of synthetic aperture imaging on a hand-held device," *IEEE International Ultrasonics Symposium, IUS*, pp. 2177–2180, 2014.
- [15] C. L. Palmer and O. M. Rindal, "Wireless, Real-Time Plane-Wave Coherent Compounding on an iPhone: A Feasibility Study," *IEEE Trans. Ultrason., Ferroelectr., Freq. Control.*, vol. 66, no. 7, pp. 1222–1231, 2019.